Journal of Power Sources 190 (2009) 264–270

Contents lists available at ScienceDirect

Journal of Power Sources

journal homepage: www.elsevier.com/locate/jpowsour

# Effect of load, temperature and humidity on the pH of the water drained out from $H_2$/air polymer electrolyte membrane fuel cells

Aboubakr M. Abdullah[a,b], Ahmad M. Mohammad[a,b], Takeyoshi Okajima[b], Fusao Kitamura[b], Takeo Ohsaka[b,*]

[a] Department of Chemistry, Faculty of Science, University of Cairo, Giza 12613, Egypt
[b] Department of Electronic Chemistry, Interdisciplinary Graduate School of Science and Engineering, Tokyo Institute of Technology, 4259-G1-05 Nagatsuta, Midori-ku, Yokohama 226-8502, Japan

ARTICLE INFO

*Article history:*
Received 4 August 2008
Received in revised form
28 December 2008
Accepted 13 January 2009
Available online 22 January 2009

*Keywords:*
PEM
Degradation
Emissions
pH
Temperature
Relative humidity

ABSTRACT

The effect of the operating conditions, e.g., load, temperature, relative humidity (RH), and the MEA's aging condition on the pH of the water drained out from the cathode and anode sides of a $H_2$/air PEM fuel cell was studied. Also the effect of the pollutants' existence in natural air on the measured pH and the performance of the fuel cell was investigated. pH values as low as 1 were measured for the water drained out from the cathode side under a low temperature–low RH condition. Increasing the load, temperature or RH value resulted in an increase of the measured pH except for the low temperature–low RH condition where increasing the load resulted in a decrease in the measured pH. On the other hand, the pH value of the water drained out from the anode side was around 4 under the same low temperature–low RH condition. Aging of the MEA at 90 °C and RH of 100% for at least 30 h resulted in low measured pH values for the water drained out from the cathode side. The polarization behaviors of the cathode under these different conditions were measured and correlated to the pH change and the performance of the MEA. Measuring the pH using a flow pH meter for the water droplets drained out from the cathode side can be used as an alarm for the onset of the chemical degradation of the Nafion membrane.



## 1. Introduction

Fuel cells are getting more attention nowadays for many reasons including the energy crisis that the world might face in the near future and the environmental impact of the increasing amount of $CO_2$ in the atmosphere which is tightly connected to the global warming problem. Fuel cells, including the polymer electrolyte membrane (PEM) fuel cell, produce only heat and water as wastes as a result of the oxidation of the hydrogen gas and the reduction of the oxygen gas according to the following reactions:

$$H_2 \rightarrow 2H^+ + 2e^-, \quad E^\circ = 0\,\text{V vs. SHE} \tag{1}$$

$$O_2 + 4H^+ + 4e^- \rightarrow 2H_2O, \quad E^\circ = 1.23\,\text{V vs. SHE} \tag{2}$$

The main problems that prevent PEM fuel cells from the commercialization until now are the durability of the membrane electrode assembly (MEA) and its cost. While the department of energy's (DOE) performance target for the PEM fuel cells for year 2010 is 5000 h (with 20,000 starts/stops) at \$45 $kW^{-1}$ for automotive stacks and 40,000 h for the stationary power plants at \$400–750 $kW^{-1}$, the engineering requirements are the operation at elevated temperatures and lower humidities at ambient pressures and the latter is a good recipe for the performance degradation [1,2]. In fact, the durability that supports the above requirements has not been achieved yet.

The decrease of the PEM fuel cells's performance with time is attributed either to the degradation of one or more of the cell components [3–9] and/or to the decrease of the catalytic activity [10,11].

Recent work on the oxygen reduction reactions confirmed the production of a large amount of hydrogen peroxide at the Pt/C interface [1,12–18]:

$$O_2 + 2H^+ + 2e^- \rightarrow H_2O_2, \quad E^\circ = 0.695\,\text{V vs. SHE} \tag{3}$$

Contrary to the reports that estimated that the amount of $H_2O_2$ produced at potentials between 0.6 and 0.8 V is less than 1% [19,20]. Inaba et al. reported a 20% production of $H_2O_2$ at a catalyst load of 5.7 $\mu g\,cm^{-2}$ [18,21].

Formation of hydrogen peroxide is reported to be one of the major problems of PEM fuel cells since it causes either a deterioration of the membrane [1] through: (i) the formation of hydroxyl and hydroperoxyl radicals which react with the perfluorosulfonic acid type ionomer in the electrode and the membrane to produce hydrofluoric acid [1] or (ii) the lowering of the catalytic activity

* Corresponding author. Tel.: +81 45 924 5404; fax: +81 45 924 5489.
*E-mail address:* Ohsaka@echem.titech.ac.jp (T. Ohsaka).

0378-7753/$ – see front matter © 2009 Elsevier B.V. All rights reserved.
doi:10.1016/j.jpowsour.2009.01.034

because of the agglomeration of the Pt particles [16,18] or the deterioration of the catalyst support [16].

The local environment within a fuel cell, e.g., temperature, humidity, pH, water distribution, membrane resistance might have direct effects on the kinetics of the electrode reactions since under the operating conditions, it is reported that the distribution of these parameters is non-uniform [22–26]. In our previous work, the local temperature distribution within a segmented fuel cell was discussed [27]. It is worthy to mention that enough attention is not being paid to study the pH change of the water drained out from the fuel cell. In fact, measuring the pH might give an indication about the performance of the fuel cell under operation and help in estimating the life time of the MEA.

In the absence of sulfur and nitrogen gaseous pollutants, a decrease in the pH can be expected as a result of the following reactions:

$$2R_f\text{–}CF_2COOH + {}^{\bullet}OH \rightarrow R_f\text{–}CF_2{}^{\bullet} + CO_2 + H_2O \quad (4a)$$

$$R_f\text{–}CF_2{}^{\bullet} + {}^{\bullet}OH \rightarrow R_f\text{–}CF_2OH \rightarrow R_f\text{–}COF + HF \quad (4b)$$

$$R_f\text{–}COF + H_2O \rightarrow R_f\text{–}CF_2OH + HF \quad (4c)$$

$$CO_2 + H_2O \rightarrow H^+ + HCO_3{}^- \quad (5)$$

Eq. (4) shows the membrane's polymer degradation by the reaction between the Nafion membrane and the OH• radicals [28]. The latter species are formed as a result of the decomposition of hydrogen peroxide molecules through their reaction with the Pt metal ions dissolved in the membrane [1,29]. Reaction (5) is the dissolution of $CO_2$ in water. In fact, electrochemical reactions that produce protons cannot be considered here since there will be no excess of $H^+$ to be released from an overall electrochemical reaction.

The aim of this work is to measure the pH change of the water drained out from the cathode and anode sides of a JARI standard PEM fuel cell as a function of load, temperature, time and relative humidity values. Also the performance of the fuel cell under study will be correlated to the pH change measured.

## 2. Experimental

MEAs and a JARI standard type fuel cell were purchased from NF Corporation, Japan. The active area of the Nafion 112 membrane is 25 $cm^2$ (5 cm × 5 cm) loaded with 1 mg $cm^{-2}$ Pt catalyst at the cathode side and 1 mg $cm^{-2}$ Pt–Ru (0.766 Pt and 0.234 Ru) at the anode side.

A PC-interfaced fuel cell system (MTB-36714) purchased from NF corporation, Japan, was used to maintain the gases' pressures, temperatures, humidity and flow rates.

The reference electrode was a reversible hydrogen electrode (RHE) with its own $H_2$ gas feed, and so it does not use the $H_2$ that passes in front of the catalyst on the anode side. This is to assure a constant hydrogen gas pressure for the reference electrode.

For the pH measurements, a flow pH meter purchased from Analyticon Inc. DKK-TOA series model number HM-30R was used to measure the pH of the water drained out from the cathode and the anode compartments. A 50 cm-long tight polyethylene tube was used between the exit of the cathode compartment and the entrance of the pH meter to assure enough cooling for the water that was drained out from the cathode side before reaching the pH meter. At high loads, the highest temperatures recorded for the water drained out from the cathode side at the entrance of pH meter were 28.7, 35.7 and 49.8 °C at the operating temperatures 50, 70 and 90 °C, respectively. It is worthy to mention that the highest temperature decreases as the operating relative humidity decreases. The pH meter was calibrated using pH buffers before each experiment and the measured pH values were corrected according to the temperature recorded by the pH meter during these measurements.

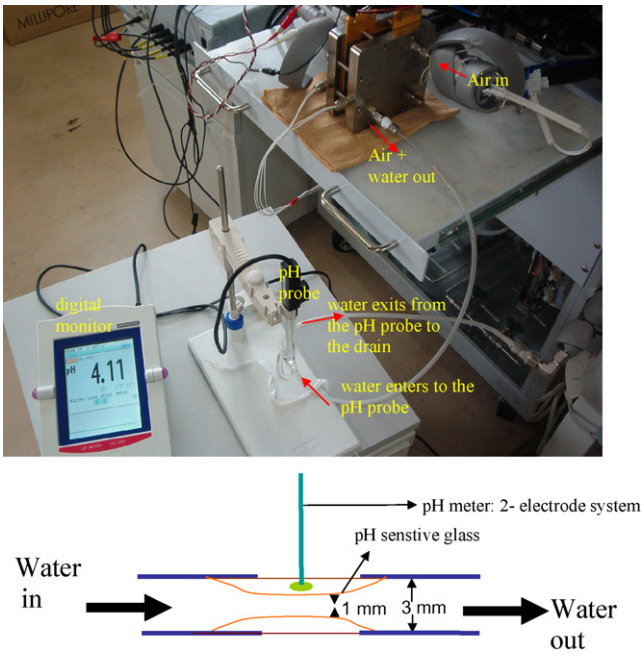


**Fig. 1.** Photograph shows the connection of the flow pH meter to the cathode side of the fuel cell. The schematic below shows the cross-section of the capillary of the flow pH meter through which the water passes along the pH sensitive glass.

Also, the pH meter was checked after the measurements were taken using the same buffers used to calibrate the pH meter before carrying out these measurements. Fig. 1 shows the experimental set up for measuring the pH of the drained water. In Fig. 1, the flow pH meter is connected to the outlet of the cathode compartment using the polyethylene tube. The schematic shows the cross-section of the capillary of the flow pH meter through which the water passes along the pH sensitive glass.

The pH of the water drained out from the anode compartment was measured in a separate measurement since only one pH meter was used. It is worthy to mention that pH was measured for the liquid phase of water drained out from the electrode compartments.

Two different sets of electrochemical measurements were designed to show the dependence of the measured pH on the load, temperature, time and relative humidity value. Galvanodynamic polarization curves (*E*–*i* curves; *E* is the cathode potential vs. RHE, *i* is the current density) were measured by polarizing the cathode at different loads starting from 0 mA $cm^{-2}$ (open circuit potential) to the load corresponding to 0 V vs. RHE which changes depending upon the temperature, the applied relative humidity and the MEA aging condition. The pH values were measured simultaneously every minute during the galvanodynamic measurements. Each pH curve is consisted of 40 points on average. The current scan rate was 0.5 A $min^{-1}$. Galvanodynamic polarization curves were measured at three different cell temperatures (50, 70 and 90 °C) and three different relative humidity values (35, 60 and 100%).

The other sets of electrochemical measurements were galvanostatic polarization curves (*E*–*t* curves) which were measured for 1 h at four different loads; 0.01, 0.1, 0.4 and 0.68 A $cm^{-2}$. These loads correspond to small, medium and big loads. Also, during these galvanostatic polarization measurements, the pH was measured simultaneously every minute with the potential of the cathode. Temperature of the galvanostatic measurements was 50 °C and the RH value was 35%.

To check the effect of pollutants in the natural air on the pH of the water drained out from the cathode compartment, a pure artificial air was used (80% $N_2$ + 20% $O_2$). Purity of the artificial air was 99.9995%.

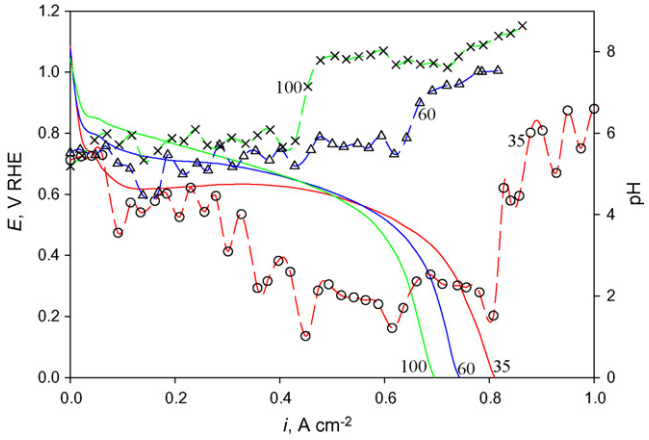


**Fig. 2.** Variation of *E* and pH as a function of the current density at a temperature of 50 °C. Red, blue and green lines are for RH values of 35, 60 and 100%, respectively. Solid lines represent *i*–*E* curves while dashed lines represent the *i*–pH ones. (For interpretation of the references to color in this figure legend, the reader is referred to the web version of the article.)

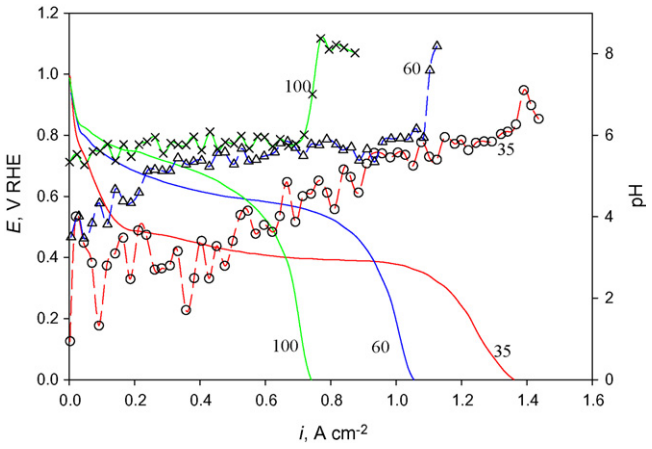


**Fig. 3.** Variation of *E* and pH as a function of the current density at a temperature of 70 °C. Red, blue and green lines are for RH values of 35, 60 and 100%, respectively. Solid lines represent *i*–*E* curves while dashed lines represent the *i*–pH ones. (For interpretation of the references to color in this figure legend, the reader is referred to the web version of the article.)

The effect of aging on the pH of the water drained out from the cathode compartment was checked by comparing the pH values measured before and after aging of the MEA. Aging of the MEA was done by cycling the galvanodynamic polarization between the OCP and the hydrogen reduction potential (0 V vs. RHE) for 30 h at 90 °C and RH of 100%.

The gases' flow rates were kept constant during all the measurements at 300 and 1000 $cm^3\ min^{-1}$ for $H_2$ and air, respectively. The gas pressures were kept constant accordingly at 1.5 and 25.3 kPa for $H_2$ and air, respectively. $H_2$ and air flew oppositely to each other.

## 3. Results and discussion

### 3.1. pH measurements during galvanodynamic polarization

Figs. 2–4 are galvanodynamic polarization–pH curves at three different temperatures of 50, 70 and 90 °C that show the performance of the fuel cell and the dependence of the measured pH of the water drained out from the cathode side upon the applied load. In each figure, the aforementioned relationships were studied at three different RH values of 35, 60 and 100%. Comparing these three figures gives some remarks that are worthy to be mentioned.

#### 3.1.1. General remarks

1. For the *i*–*E* curves in Figs. 2–4, at low RH values, the performance of the cathode is better at higher loads. This was attributed to the increase of the amount of water produced at these loads. On the other hand, at high RH values, the increase in the load led to flooding which resulted in a decrease in the performance.
2. At any temperature, the OCP increases as the RH decreases. The values of OCP at different temperatures and RH values are summarized in Table 1. This was attributed to the decrease of the gases' crossover [30] as the water content decreases, i.e., as the RH decreases [31].

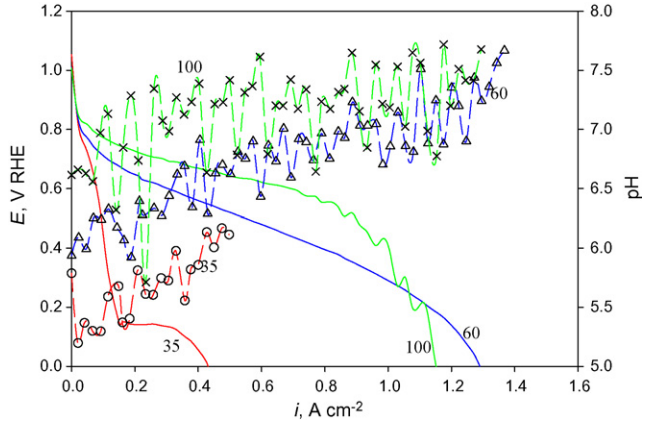


**Fig. 4.** Variation of *E* and pH as a function of the current density at a temperature of 90 °C. Red, blue and green lines are for RH values of 35, 60 and 100%, respectively. Solid lines represent *i*–*E* curves while dashed lines represent the *i*–pH ones. (For interpretation of the references to color in this figure legend, the reader is referred to the web version of the article.)

#### 3.1.2. pH measurements

3. From Figs. 2–4, it can be noticed that the lower is the RH value, the lower the pH is. In Fig. 2, the pH was around 2 for the loads ranging from 0.4 to 0.8 A $cm^{-2}$ at an RH value of 35%. Increasing the RH to 60% resulted in an increase of the pH to around 5 which further increased to 6 in the case of the RH value of 100%. The same behavior was noticed at the higher temperatures in Figs. 3 and 4.
4. Increasing the temperature resulted in an increase of the measured pH regardless of the value of RH. For example, at an RH value of 35%, the pH increased from 2 at a temperature of 50 °C to 5.5 at a temperature of 90 °C (compare Figs. 2 and 4).
5. An argument regarding whether the measured low pH values are load-dependent or water flow rate-dependent can be raised here. To resolve this argument the load was scanned from 0 A $cm^{-2}$ to

**Table 1**
Open circuit potential change as a function of temperature and RH.

| | *T* = 50 °C | | | *T* = 70 °C | | | *T* = 90 °C | | |
|---|---|---|---|---|---|---|---|---|---|
| | RH 35% | RH 60% | RH 100% | RH 35% | RH 60% | RH 100% | RH 35% | RH 60% | RH 100% |
| OCP, V vs. RHE | 1.085 | 1.074 | 1.043 | 0.994 | 0.987 | 0.939 | 1.053 | 1.011 | 1.008 |

the load corresponding to 0 V then it was scanned in the reverse direction to 0 A cm$^{-2}$. During this cyclic polarization, the pH was measured every minute (data not shown here). During the forward scan, it was found that the pH started to decrease at 736 mV and continued to decrease until it reached pH 1 at 0 V. On the reverse scan, pH continued to be low until the potential reached 649 mV then it started to increase again. At OCP the pH was 2.41. Waiting for 20 min raised the pH to its initial value (4.5). This indicates that the pH is load-dependent and not water flow rate-dependent since at high flow rates of water (high loads) where more dilution for the produced $H^+$ takes place the pH was low. On the other hand at low flow rates of water (small loads) where the produced protons are concentrated in small amount of water, the pH was high.

The question now is which reaction among those listed as Eqs. (4) and (5) are responsible for low pH values shown in these figures.

### 3.1.3. Effect of pollutants on the pH measurements

6. Fig. 5 compares the pH measurements of the water drained out from the cathode side with the polarization behavior of the same cathode at a temperature of 50 °C and an RH value of 35% in the case of using natural and artificial (pure) air. The polarization curves are almost identical which indicates that the kinetics of the ORR was not actually affected by the quality of the air. Also, the difference in the measured pH values is within 1 pH unit on average at small loads while at higher loads there is almost no difference. This small difference in pH suggested that, in this case, the presence of $CO_2$ and $SO_2$, if any, in the air did not affect the pH measurements significantly. In brief, Reaction (5) should be excluded at least as a major reason for these low measured pH values.

### 3.1.4. Role of $H_2O_2$ production in lowering the pH

7. Among the two reactions listed in Eqs. (4a–c) and (4) and (5), only the polymer membrane degradation (Reaction (4)) is not yet discussed. Sethuraman et al. reported that the rate of $H_2O_2$ formation at the anode side is three orders of magnitude lower than that at the cathode side [1]. It is worthy to mention here that the pH of the water drained out from the anode side was also around 3 pH units higher than that drained out from the cathode side at the same conditions (compare Figs. 2 and 6). The average pH value measured for the water drained out from the cathode at a temperature of 50 °C and an RH of 35% was 1.8, while it was around 4.8 in the case of the water drained out from the anode side. This supports the idea that $H_2O_2$ formation might be the reason for the observed low pH. They also have found that $H_2O_2$ selectivity in the ORR increases as the water activity decreases (RH decreases) [1], which agrees with the present observations, i.e., the lower the RH is, the lower is the pH of the water drained out from the cathode side.

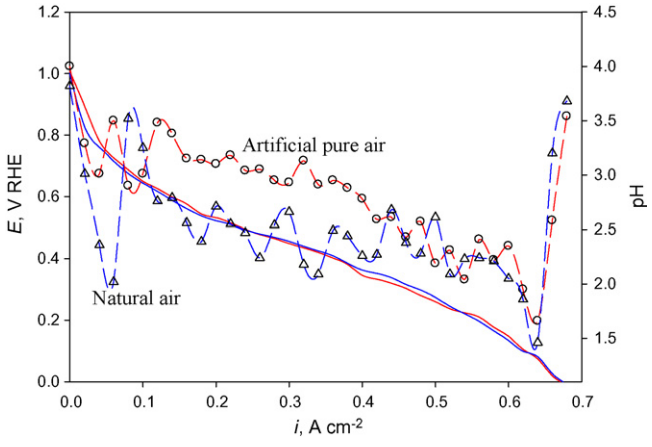


**Fig. 5.** Effect of pollutants on the polarization behavior and the pH drained out from the cathode compartment of the fuel cell at a temperature of 50 °C and an RH value of 35%. Red line is for the artificial pure air while the blue one is for the natural air. Solid lines represent polarization behavior and dashed lines represent the measured pH.

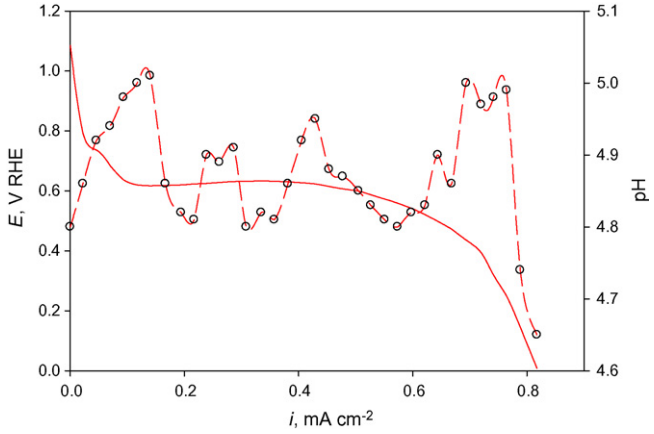


**Fig. 6.** Variation of $E$ and the pH of the water drained out from the anode side as a function of the current density at a temperature of 50 °C and an RH value of 35%. The solid line represents $i$–$E$ curve while dashed line represents the $i$–pH one.

8. The role of $H_2O_2$ in lowering the pH is based upon its decomposition to OH• radicals by reacting with the Pt metal ions dissolved in the membrane [1,29] (from corrosion of the catalyst), and $Ni^{2+}$, $Fe^{2+}$ and $Fe^{3+}$ (from corrosion of the stainless steel end plates). These OH• radicals attack the membrane causing its degradation and the production of HF which decreases the measured pH (see Eq. (4)). It is worthy to mention that the increase of the concentration of these cations increases the amount of the OH• radicals which increases the rate of degradation of the Nafion membrane.
9. The cations formed as a result of the corrosion of the stainless steel end plates undergo a hydrolysis which lowers the pH to values less than the p$K_a$'s for HF (3.19) and $H_2CO_3$ (6.4). Hydrolysis of $Fe^{3+}$ can lower the pH value to 1.5 [32] which is close to the value measured in Fig. 2.
10. Another reason that might be responsible for lowering the pH to values less than 3, as shown in Fig. 2, is the oxidation of $SO_2$ gas that is formed as a result of the chemical degradation of Nafion membranes. The oxidation of $SO_2$ and $H_2SO_3$ to sulfuric acid is reported by Zhdanov [33] to be around 0.17 V. This potential is very close to the potential where low pH values were measured (see Fig. 2). It is worthy to mention here that the source of $SO_2$ gas is the degraded Nafion membrane, but not the natural air. This can be confirmed from Fig. 5 where the measured pH was very low without depending on whether the natural air or the artificial pure air is used.
11. Xie et al. reported the existence of fluoride anions in the cathode outlet water which confirms the degradation of Nafion 112 membrane or the catalyst-layer recast ionomer, or both [34].
12. Generally the pH increases as the load increases except for the low RH at 50 °C in Fig. 2. The exception shown in Fig. 1, i.e., the pH continues to decrease as the load increases, is attributed to the lower temperature and lower RH because the $H_2O_2$ selectivity in the ORR increases at low RH [1] and at the same time $H_2O_2$ molecules can resist the decomposition at low temperatures [35,36].

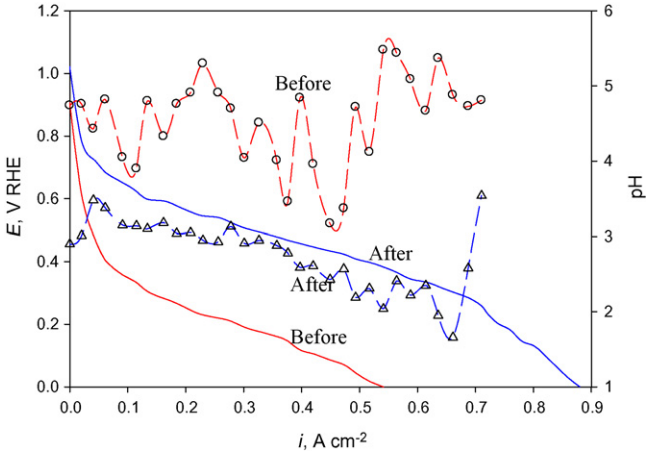


**Fig. 7.** Effect of aging on the change of $E$ (solid lines) and pH (dashed lines) as a function of the current density at a temperature of 50 °C and an RH value of 35%. Red and blue colors are designated for before aging and after aging, respectively. (For interpretation of the references to color in this figure legend, the reader is referred to the web version of the article.)

13. Although, measuring the pH can be used as an alarm for the onset of the Nafion membrane degradation, the rate of the chemical degradation is difficult to be estimated from measuring the pH alone because the pH is a concentration term rather than a production rate term that depends on the local operating parameters, e.g., temperature and RH. Comparing the pH measurements at the same operating conditions with the fuel cells that do and do not suffer from chemical degradation of their Nafion membranes will decide whether the degradation is taking place or not. Also comparing the pH measurements with other characteristics like fluoride ions release rate (FRR) and sulfate ions release rate (SRR) might be very useful in estimating the rate of chemical degradation of the Nafion membranes.

### 3.1.5. Aging effect

The measured pH does not go lower than 3 as long as the MEAs are underaged. When the membrane was aged for enough time (30 h at 90 °C and an RH value of 100%) and then it was used at lower temperatures and lower RH values, the pH of the water drained out from the cathode side was found to decrease dramatically. Fig. 7 shows the effect of aging of the MEA on the pH of the water drained out from the cathode compartment. The MEA was aged by polarizing the fuel cell galvanodynamically at a slow scan rate of 60 mA min$^{-1}$ for 10 h starting from the OCP (≈1 V vs. RHE) down to the nominal reduction potential of hydrogen. The operating conditions of the fuel cell during this aging process were a temperature of 90 °C and an RH value of 100%. At the end of the galvanodynamic polarization, the fuel cell was allowed to cool down to the room temperature at the OCP. This process was repeated three times for a total aging time of 30 h. Comparing the measured pH before and after this aging process reveals that the aging process increases the acidity of the water drained out from the fuel cell's cathode outlet. In fact, the aging process might increase the amount of $Pt^{2+}$, $Fe^{2+}$, $Fe^{3+}$ and $Ni^{2+}$ significantly within the membrane (especially $Fe^{2+}$ and $Fe^{3+}$). The role of these cations is twofold: first, they enormously suppress the charge transfer step in the oxygen reduction reaction (ORR) that occurs at the Pt–ionomer interface [37] which might increase the selectivity of $H_2O_2$ formation. It is worthy to mention here that these cations do not affect the charge transfer step in the ORR at the normal Pt–electrolyte solution interface [38]. Therefore, in the presence of high concentrations of these metallic ions, the concentration of the formed HO• and HOO• radicals is much higher (since their formation depends on the presence of these transition metal cations and the $H_2O_2$ molecules) and the degradation is significantly enhanced as the load increases and consequently more $H_2O_2$ molecules are formed. This agrees with the conclusions reported in the literature [28] that cycling of load, temperature, and RH can result in an increase of the degradation rate by several orders of the magnitude. Also, these cations, especially $Fe^{3+}$ can be hydrolyzed and this lowers the measured pH significantly to values close to 1. In addition, the temperature cycling during the aging process might increase the production of $SO_2$ from the degraded membrane which is oxidized to sulfuric acid at potentials around 0.17 V and the latter product is responsible for measuring these very low pH values (less than 3).

Attributing the aging effect to the surface change of the Pt catalyst is another possibility. Song et al. reported the change of the Pt surface from Pt/PtO at low loads to pure Pt at high loads [39]. Also the effect of RH cannot be denied as the degree of Pt oxidation increases significantly with an increase in RH from 20 to 72% [40]. The decrease in the Pt active area due to agglomeration at elevated temperatures and high RH values which results in a significant generation of the peroxide especially when the PEM fuel cell operates at low temperature–low RH conditions might be another reason for the remarkable aging effect on the measured pH of the water drained out from the cathode compartment [41]. Wei et al. reported an agglomeration of the Pt nanoparticles at 95 °C where the particle's size increases from 7.5 to 12.2 nm [42].

### 3.2. pH measurements during galvanostatic polarization

Figs. 8–11 show the galvanostatic polarization behavior of the cathode at different current densities at 50 °C for 1 h and the pH change during the polarization. These experiments were conducted to examine the change of pH at a constant long loading and to compare the results with the galvanodynamic polarization measurements mentioned in the previous section. Several remarkable points can be noticed by comparing the different curves:

1. Comparing the solid lines in Fig. 2 ($i$–$E$ curves at different RH values) and Figs. 8–11 ($E$–$t$ curves at different loads and RH values), an agreement between the galvanostatic and the galvanodynamic measurements can be noticed where the performance at small loads is better at higher RH conditions and vice versa. This can be seen clearly by comparing the potentials at a certain load: the higher is the potential (lower overpotential), the better the performance is.

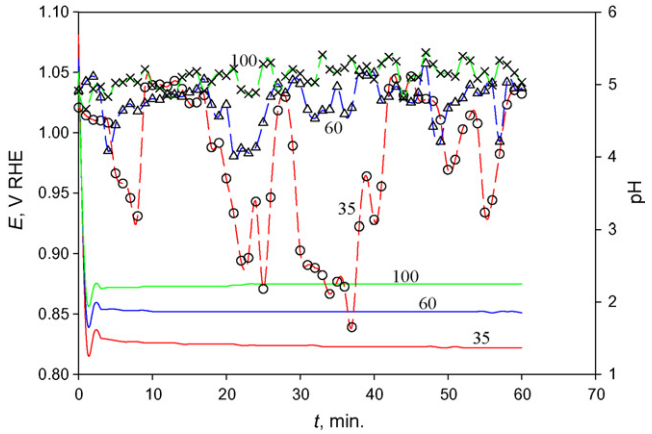


**Fig. 8.** Transient change of $E$ and pH while a load of 0.01 A cm$^{-2}$ was applied at a temperature of 50 °C for 1 h. Red, blue and green lines are for RH values of 35, 60 and 100%, respectively. Solid lines correspond to $E$ while dashed lines correspond to pH. (For interpretation of the references to color in this figure legend, the reader is referred to the web version of the article.)

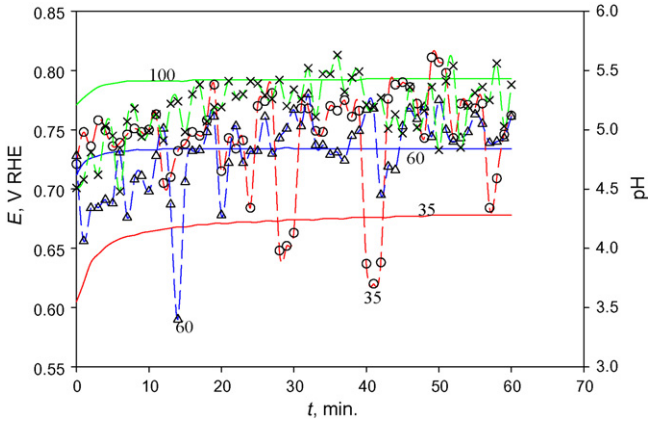


**Fig. 9.** Transient change of $E$ and pH while a load of 0.1 A cm$^{-2}$ was applied at a temperature of 50 °C for 1 h. Red, blue and green lines are for RH values of 35, 60 and 100%, respectively. Solid lines correspond to $E$ while dashed lines correspond to pH. (For interpretation of the references to color in this figure legend, the reader is referred to the web version of the article.)

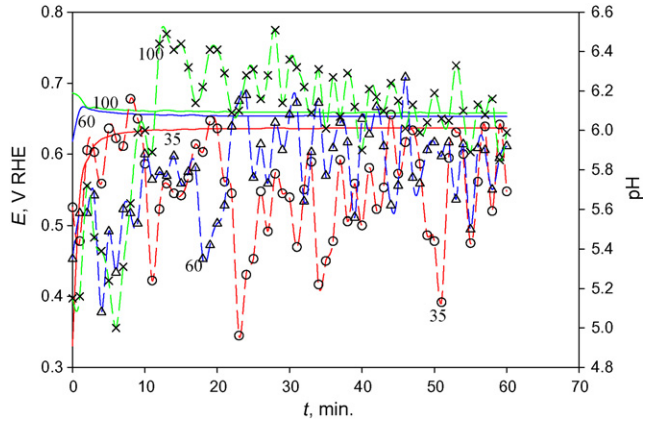


**Fig. 10.** Transient change of $E$ and pH while a load of 0.4 A cm$^{-2}$ was applied at a temperature of 50 °C for 1 h. Red, blue and green lines are for RH values of 35, 60 and 100%, respectively. Solid lines correspond to $E$ while dashed lines correspond to pH. (For interpretation of the references to color in this figure legend, the reader is referred to the web version of the article.)

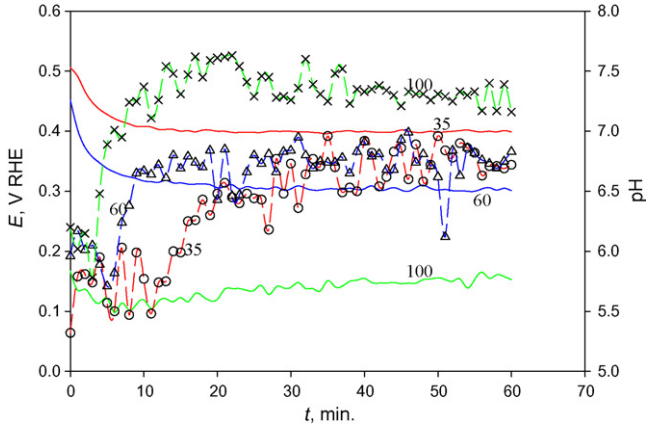


**Fig. 11.** Transient change of $E$ and pH while a load of 0.68 A cm$^{-2}$ was applied at a temperature of 50 °C for 1 h. Red, blue and green lines are for RH values of 35, 60 and 100%, respectively. Solid lines correspond to $E$ while dashed lines correspond to pH. (For interpretation of the references to color in this figure legend, the reader is referred to the web version of the article.)

2. The transient pH measurements at constant loads (Figs. 8–11) also have good agreement with the pH measurements (shown in Figs. 2–4) during the galvanodynamic polarization of the cathodes between the OCP and the nominal hydrogen reduction potential (≈0 V vs. RHE) where the higher is the applied load, the higher the measured pH is.
3. The relation between the RH and the pH is also confirmed from these figures. Comparing them, it can be easily noticed that the pH at RH of 100% is (green dashed lines) always higher than the pH at RH of 35 and 60% (red and blue dashed lines).
4. At a constant load, at any RH value and under any working temperature, the pH is not constant but it "oscillates" over several pH units. The difference between the minimum and maximum pH values recorded for these oscillations decreases as the RH increases. This might be attributed to the increase of the amount of water drained out from the cathode as the RH increases. In addition, the average value of the oscillating pH is almost constant at a certain load, RH and temperature, and this average pH increases as the RH increases which is attributed to the decrease in $H_2O_2$ selectivity in the ORR as RH increases [1]. The oscillation of the pH might be mainly attributed to the change in the local pH, temperature and RH where the stability of $H_2O_2$ decreases as the pH and temperature increases and its selectivity decreases as the RH increases.
5. As the local RH value increases, the pH increases and vice versa. This leads to the noticed oscillation behavior. The decrease in the magnitude of the pH oscillation with increasing the RH value might be attributed to the smaller change in the local RH value as the operating RH value increases. At low operating RH value, on the other hand, the local RH can change (increase or decrease) dramatically which results in big pH spikes. The change in the transient RH value and the transient distribution of temperature within an operating fuel cell are interrelated.
6. When the loads and the RH values are small (Fig. 8), the low pH regions in the pH spikes continue for a long time while the oscillating pH reaches the higher values. Generally, as the load increases, the low pH regions do not last for a long time.

## 4. Conclusions and summary

The measured low pH of the water drained out from the cathode compartment is attributed to the production of $H_2O_2$ molecules which decompose to form HO• radicals which attack the Nafion membrane. The effect of the pollutants existing in the natural air is small compared to the effect of $H_2O_2$ production. The measured pH was directly correlated to the operating conditions of the fuel cell. Lowering the temperature (50 °C) and the relative humidity (RH 35%) resulted in a very acidic water drained out from the cathode compartment (pH 1) at small loads. As the load increases the pH increases regardless of the working conditions except for the low temperature–low RH condition. The reason for this is attributed to the increase of the $H_2O_2$ selectivity in the ORR at low RH values and the stability of $H_2O_2$ molecules at lower temperatures. At a constant load, the pH oscillates. The reason for this oscillation might be attributed to the local change in the temperature, pH and RH values. The pH of water drained out from the anode compartment was much higher than that drained out from the cathode compartment as a result of the difference in the amount of hydrogen peroxide produced, i.e., the amount of $H_2O_2$ produced at the cathode side is by three orders of magnitude more than that at the anode side. Aging of the MEA has a direct effect on the measured pH. Underaged MEAs did not support pH values lower than 3. On the other hand, the aged MEAs resulted in a measured pH as low as 1. The reason for this might be attributed to the corrosion of the end plates and bipolar plates, releasing $Fe^{2+}$ and $Fe^{3+}$ cations, at high

temp.–high RH condition during the aging process. These cations suppress the charge transfer at the Pt–ionomer interface and this increases the selectivity of $H_2O_2$ in the ORR. The agglomeration of the Pt nanoparticles that can take place during the aging process also results in an increase in the amount of $H_2O_2$ produced during the ORR. In addition, $Fe^{3+}$ cations undergo hydrolysis which lowers the pH to values close to 1. Also the oxidation of $SO_2$ and $H_2SO_3$ at potentials close to 0.17 V might be another reason for lowering the measured pH to values lower than 3. In brief, degradation of the polymer membrane is the most influencing process that results in a decrease in the pH of the water drained out from the cathode and anode compartments. It is also important to notice that operating the fuel cell at a low RH–low temperature conditions after being operated at high RH–high temperature conditions has detrimental effects on the fuel cells' MEAs. Measuring the pH of the drained water can be used as an alarm for the onset of the chemical degradation of Nafion membranes. Correlating the measured pH with the fluoride ions release rate (FRR) and the sulfate ions release rate (SRR) may be capable of using the pH measurements as a quantitative tool to estimate the chemical degradation of Nafion membranes.

## Acknowledgements

This work was financially supported by the Ministry of Education, Culture, Sports, Science and Technology (MEXT), Japan and also by New Energy and Industrial Technology Development Organization (NEDO), Japan.

## References

[1] V.A. Sethuraman, J.W. Weidner, A.T. Haug, S. Motupally, L.V. Protsailo, J. Electrochem. Soc. 155 (2008) B50.
[2] H. Xu, H.R. Kunz, J.M. Fenton, Electrochim. Acta 52 (2007) 3525.
[3] M. Schulze, N. Wagner, T. Kaz, K.A. Friedrich, Electrochim. Acta 52 (2007) 2328.
[4] K. Teranishi, K. Kawata, S. Tsushima, S. Hirai, Electrochem. Solid-State Lett. 9 (2006) A475.
[5] M. Cai, M.S. Ruthkosky, B. Merzougui, S. Swathirajan, M.P. Balogh, S.H. Oh, J. Power Sources 160 (2006) 977.
[6] D.A. Stevens, J.R. Dahn, Carbon 43 (2005) 179.
[7] V.A. Sethuraman, J.W. Weidner, A.T. Haug, L.V. Protsailo, J. Electrochem. Soc. 155 (2008) B119.
[8] W. Bi, G.E. Gray, T.F. Fuller, Electrochem. Solid-State Lett. 10 (2007) B101.
[9] X. Wang, R. Kumar, D.J. Myers, Electrochem. Solid-State Lett. 9 (2006) A225.
[10] M.S. Wilson, F.H. Garzon, K.E. Sickafus, S. Gottesfeld, J. Electrochem. Soc. 140 (1993) 2872.
[11] M. Schulze, A. Schneider, E. Gulzow, J. Power Sources 127 (2004) 213.
[12] L. Zhang, S. Mukerjee, J. Electrochem. Soc. 153 (2006) A1062.
[13] M. Inaba, T. Kinumoto, M. Kiriake, R. Umebayashi, A. Tasaka, Z. Ogumi, Electrochim. Acta 51 (2006) 5746.
[14] F. Dundar, A. Smirnova, X. Dong, A. Ata, N. Sammes, J. Fuel Cell Sci. Technol. 3 (2006) 428.
[15] T. Kinumoto, M. Inaba, Y. Nakayama, K. Ogata, R. Umebayashi, A. Tasaka, Y. Iriyama, T. Abe, Z. Ogumi, J. Power Sources 158 (2006) 1222.
[16] T. Kinumoto, K. Takai, Y. Iriyama, T. Abe, M. Inaba, Z. Ogumi, J. Electrochem. Soc. 153 (2006) A58.
[17] L.M. Roen, C.H. Paik, T.D. Jarvi, Electrochem. Solid-State Lett. 7 (2004) A19.
[18] M. Inaba, H. Yamada, J. Tokunaga, A. Tasaka, Electrochem. Solid-State Lett. 7 (2004) A474.
[19] U.A. Paulus, T.J. Schmidt, H.A. Gasteiger, R.J. Behm, J. Electroanal. Chem. 495 (2001) 134.
[20] O. Antoine, R. Durand, J. Appl. Electrochem. 30 (2000) 839.
[21] M. Inaba, M. Ando, A. Hatanaka, A. Nomoto, K. Matsuzawa, A. Tasaka, T. Kinumoto, Y. Iriyama, Z. Ogumi, Electrochim. Acta 52 (2006) 1632.
[22] X. Yan, M. Hou, L. Sun, H. Cheng, Y. Hong, D. Liang, Q. Shen, P. Ming, B. Yi, J. Power Sources 163 (2007) 966.
[23] J.J. Hwang, S.J. Liu, J. Power Sources 162 (2006) 1203.
[24] Z. Siroma, A. Nishikawa, R. Kitayama, S. Koge, K. Yasuda, in: H.I. Honolulu, M. Murthy, K. Ota, J.W. Van Zee, S.R. Narayanan, E.S. Takeuchi (Eds.), The Eletrochemical Society Joint International Meeting, PV2004-21, October 3–8, 2004, p. 565.
[25] S. Shimpalee, S. Dutta, Numer. Heat Transf. A: Appl. 38 (2000) 111.
[26] C.-Y. Lee, C.-L. Hsieh, G.-W. Wu, Jpn. J. Appl. Phys. 46 (2007) 3155.
[27] A.M. Abdullah, T. Okajima, A.M. Mohammad, F. Kitamura, T. Ohsaka, J. Power Sources 172 (2007) 209.
[28] F.A. de Bruijn, V.A.T. Dam, G.J.M. Janssen, Fuel Cells 8 (2008) 3.
[29] A. Panchenko, H. Dilger, J. Kerres, M. Hein, A. Ullrich, T. Kaz, E. Roduner, Phys. Chem. Chem. Phys. 6 (2004) 2891.
[30] A. Collier, H. Wang, X. Zi Yuan, J. Zhang, D.P. Wilkinson, Int. J. Hydrogen Energy 31 (2006) 1838.
[31] J. Larminie, A. Dicks, Fuel Cell Systems Explained, John Wiley & Sons Ltd., West Sussex, England, 2003, p. 418.
[32] A.E. Martell, Coordination Chemistry, vol. I, Van Nostrand Reinhold Company, New York, 1971, p. 431.
[33] S.I. Zhdanov, in: A.J. Bard (Ed.), Encyclopedia of Electrochemistry of the Elements, vol. IV, Marcel Deckker, New York, 1975, p. 276.
[34] J. Xie, D.L. Wood III, D.M. Wayne, T.A. Zawodzinski, P. Atanassov, R.L. Borup, J. Electrochem. Soc. 152 (2005) A104.
[35] L.G. Edwards, S. Sarangapani, Proc. Electrochem. Soc. 84 (11) (1984) 254.
[36] V.R. Choudhary, P. Jana, Appl. Catal. A: Gen. 335 (2008) 95.
[37] T. Okada, Y. Ayato, J. Dale, M. Yuasa, I. Sekine, O.A. Asbjornsen, Phys. Chem. Chem. Phys. 2 (2000) 3255.
[38] T. Okada, H. Satou, M. Yuasa, Langmuir 19 (2003) 2325.
[39] C. Song, Y. Tang, J.L. Zhang, J. Zhang, H. Wang, J. Shen, S. McDermid, J. Li, P. Kozak, Electrochim. Acta 52 (2007) 2552.
[40] H. Xu, R. Kunz, J.M. Fenton, Electrochem. Solid State 10 (2007) B1.
[41] A.S. Agarwal, U. Landau, T. Zawodzinski Jr., Proc. Electrochem. Soc. (2004) 515 (PV 2004-21).
[42] Z. Wei, H. Guo, Z. Tang, J. Power Sources 62 (1996) 233.